Towards the superconductivity in $La_3Ni_2O_7$ thin films under large compressive strain.

Henri BLUM

under the supervision of :
Daniele PREZIOSI and Hoshang SAHIB

IPCMS

Université de Strasbourg

Sommaire

Introduction

1. Superconductivity is still a very active field of research.
2. The theory and concept behind high temperature (or unconventional) superconductor is still not well known.
3. new high temperature superconductors could be a huge revolution in many domains in science and engineering.

Current research on the field

1. Nickelates are close to Cuprates, well known for their superconductivity at high temperature.
2. Discovery of high temperature (80°K) superconductivity in a bulk crystal of $La_3Ni_2O_3$ under high pressure (20 GPa) - 2023 [1].

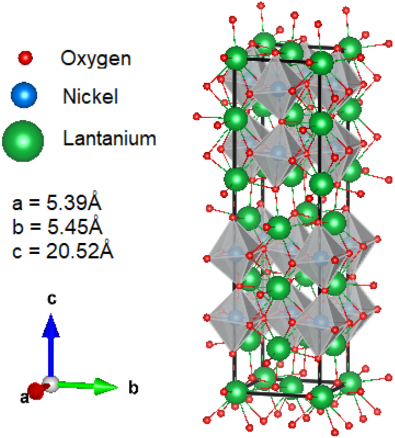

Figure 1 – Unit cell of the $La_3Ni_2O_3$ crystal. [2]

Octahedra titlting

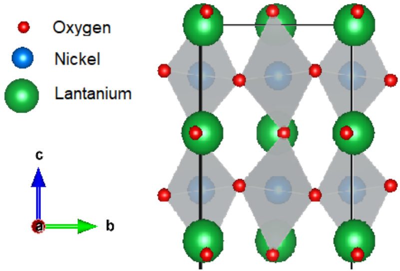

Figure 2 – Octahedra disposition in the bulk crystal of $La_3Ni_2O_7$

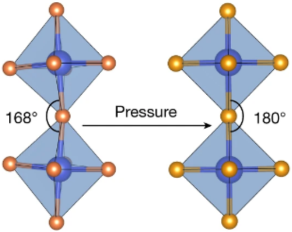

Figure 3 – The angle between two adjacent octahedra changes from 168° in the ambient-pressure to 180° in the high-pressure. from [1].

The lattices parameters

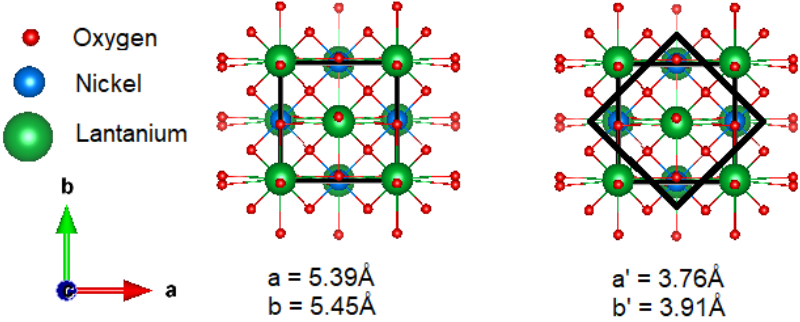

Figure 4 – Usual and diagonal in-plane lattice parameters.

The two substrates

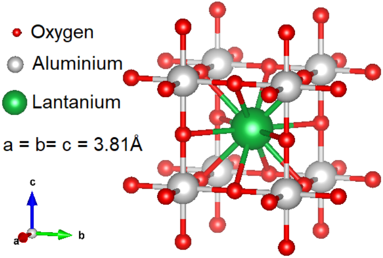

Figure 5 – Unit cell of the La Al O_3 (LAO) substrate. [3]

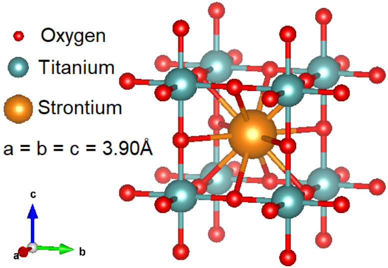

Figure 6 – Unit cell of the Sr Ti O_3 (STO) substrate. [4]

These will apply a strain on the crystal we want to grow.

$$\epsilon_{LAO} = -1.12\% \; ; \; \epsilon_{STO} = 1.88\% \text{ [5]}$$

The PLD (Pulsed Laser Deposition)

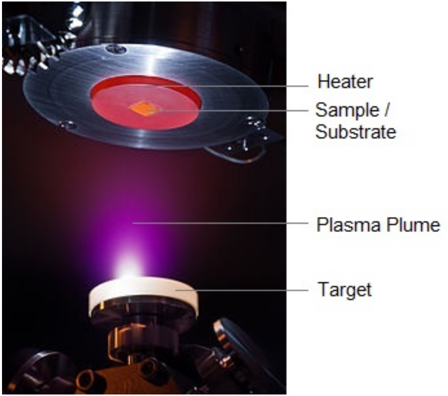

Figure 7 – Photo of the grow process of a crystal by PLD.

1. Under vacuum beside a set concentration of dioxygen, a pulsed laser in the X-ray is being shun on a target made of $La_3Ni_2O_7$.
2. The target turn into a plasma plume and will fix on the heated substrate layer by layer.
3. An electron beam reflection gives us information on the number of layer created.

Schematic of a sample

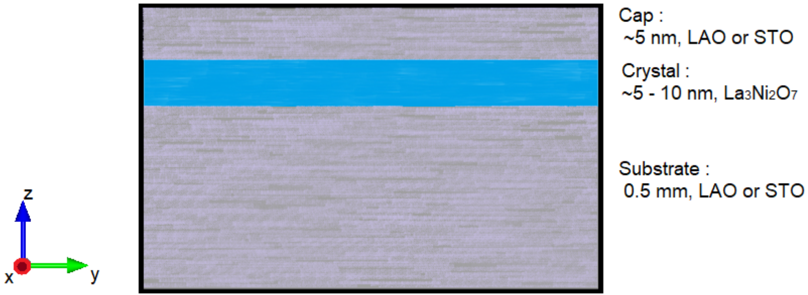

Figure 8 – drawing of the different layers of a given sample.

The AFM (Atomic force microscope)

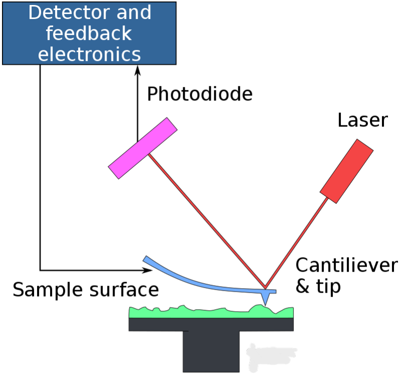

Figure 9 – Schematic of the atomic force microscope, vertical resolution in the Å.

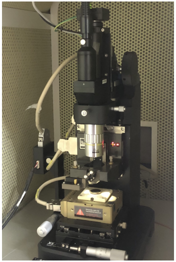

Figure 10 – Photo of the atomic force microscope.

The AFM (Atomic force microscope)

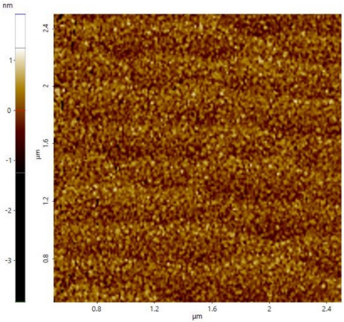

Figure 11 – Sample C (LAO substrate) topography realized with AFM, roughness = 0.28 nm.

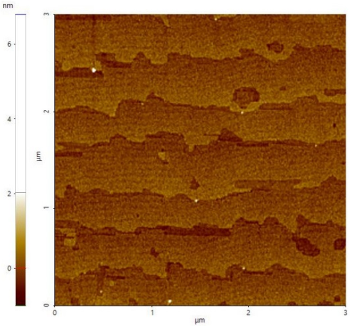

Figure 12 – Sample D (STO substrate) topography realized with AFM, roughness = 0.22 nm.

Principle of the XRD (X-Ray Diffraction)

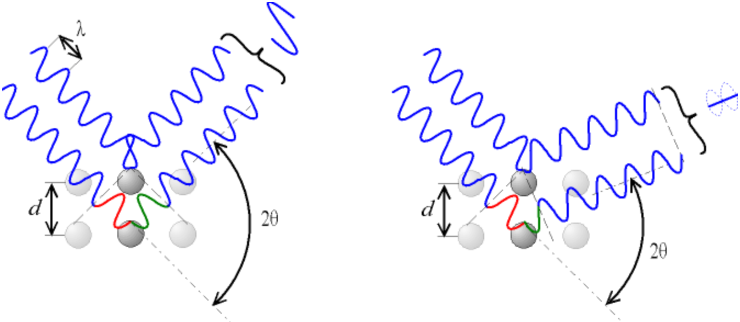

Figure 13 – Schematic of X-ray diffracting on a crystal plane following Braggs law.

$$2d \sin\theta = n\lambda\,;\ \lambda = 1.5410^{-10}\ \text{m}$$

Our results on XRD measurement - LAO substrate

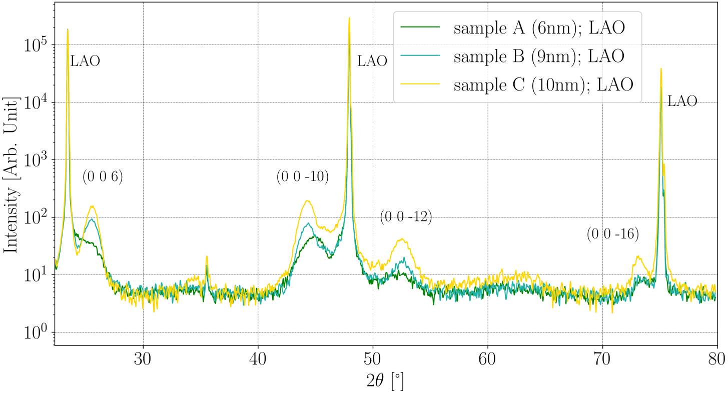

Figure 14 – Intensity versus angle for samples with different width grown on LAO substrate.

Our results on XRD measurement - STO substrate

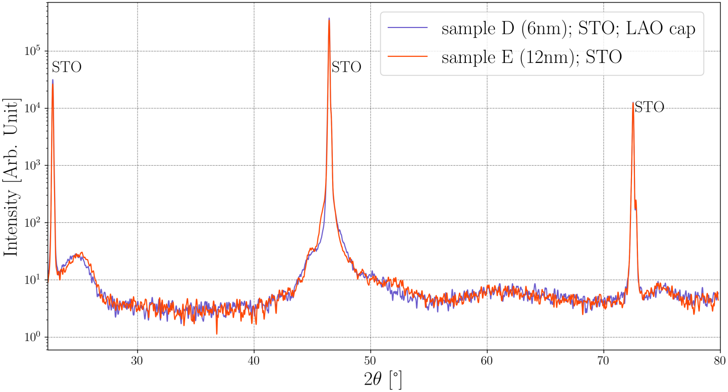

Figure 15 – Intensity versus angle for samples with different width grown on STO substrate.

Principle of the resistivity measurement

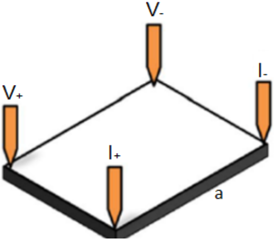

Figure 16 – Schematic of a four points resistivity measurement.

Van der Pauw measurement conditions :

1. contacts are on the circumference.
2. contacts are sufficiently small.
3. sample is homogeneous.
4. sample is singly connected (contains no holes).

Our results on conductivity measurement - LAO substrate

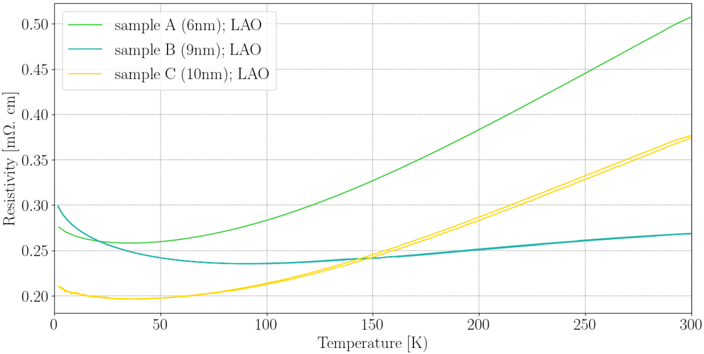

Figure 17 – resistivity versus temperature for samples with different width grown on LAO substrate.

Our results on resistivity measurement - STO substrate

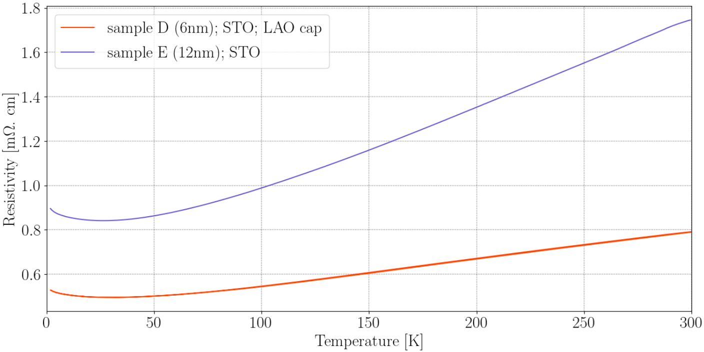

Figure 18 – resistivity versus temperature for samples with different width grown on STO substrate.

Resistivity as a power of temperature

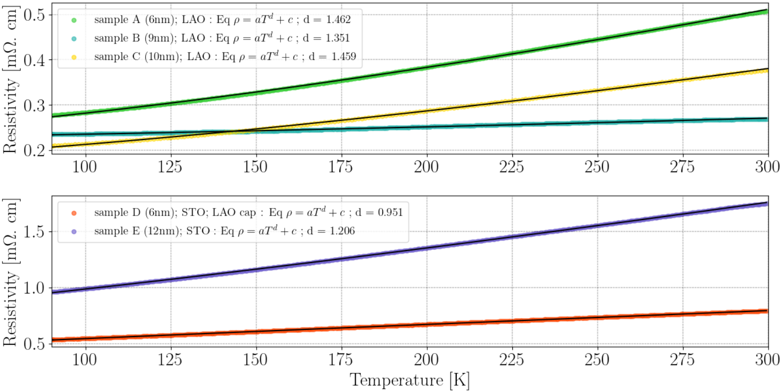

Figure 19 – Fitting of the resistivity as a power of temperature for all of our samples.

The inconclusive topotactic reduction

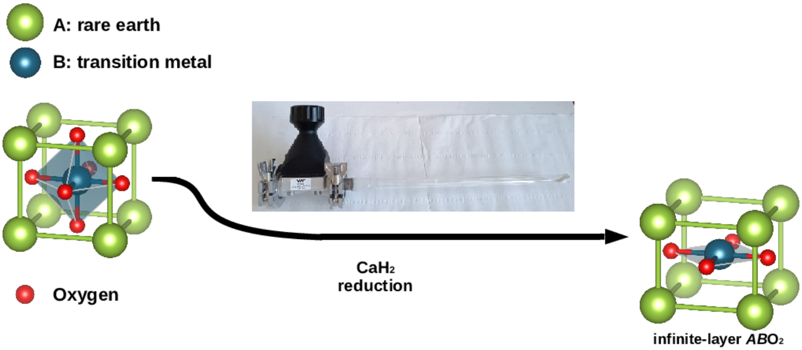

Figure 20 – Schematic of the process of the chemical topotactic reduction

Conclusion

1. traces of strange metal behavior were found in one of our samples.
2. Topotactic reduction was unable to create infinite-layer but instead seems to destroy the unit cell, perhaps through a chemical reaction.
3. To go further : we still can try to measure the conductivity of the samples under pressure like [1].

H. Sun et al.
Signatures of superconductivity near 80K in a nickelate under high pressure.
Nature, 621:493–498, 12 July 2023.

Ling C.D. et al.
Neutron diffraction study of La3 Ni2 O7 : structural relationships among n = 1, 2, and 3 phases Lan+1 Nin O3n+1.
Journal of Solid State Chemistry, 152:517–525, 2000.

Howard C.J. et al.
Neutron powder diffraction study of rhombohedral rare-earth aluminates and the rhombohedral to cubic phase transition.
Journal of Physics : Condensed Matter, 12:348–365, 2000.

Natheer B. et al.
Three Techniques Used to Produce BaTiO3 Fine Powder.
Journal of Modern Physics, 2:1420–1428, 2011.

T. Cui et al.
Strain-mediated phase crossover in RuddlesdenPopper nickelates.
ArXiv, 22 November 2023.

More about the PLD.

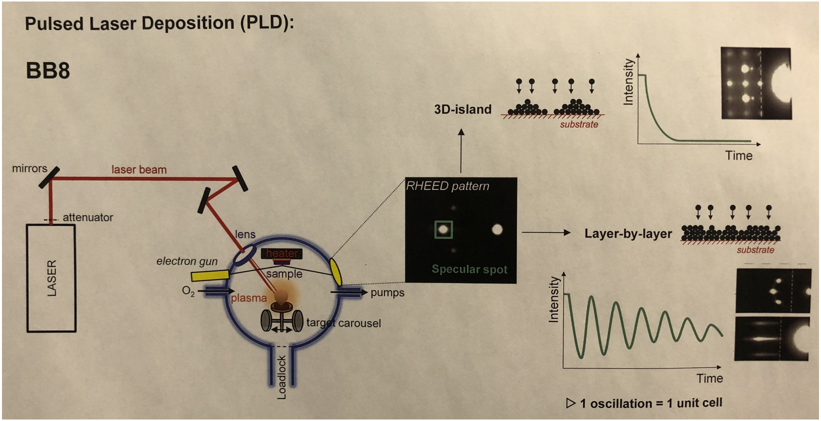

Figure 21 – Detailed sketch of the PLD and the electron beam reflection.